JOURNAL OF MATERIALS SCIENCE **35** (2000) 3923–3929

Microstructural characterization of γ-TiAl base alloy by electron probe x-ray microanalysis and electron backscatter diffraction

L. LEVIN, A. TOKAR, A. BERNER
Department of Materials Engineering, Technion - Israel Insitute of Technology, Technion-City, Haifa, 32000, Israel
E-mail: berner@tx.technion.ac.il

Electron backscatter diffraction (EBSD) and electron probe x-ray microanalysis (EPMA) in combination with x-ray diffraction (XRD) were applied for phase identification of the ternary precipitates and accompanying phases in Ti-49.6Al-1.9Fe alloy after heat treatment at 1400°C followed by furnace cooling. The heat treatment resulted in formation of the duplex structure consisting of equiaxed grains of the γ phase (AuCu type) and lamellae of the γ and α_2 (Ni_3Sn type). The ternary τ_2 ($Mn_{23}Th_6$ type) phase, containing 21–22 at. % Fe, was revealed on the grain boundaries of the γ-matrix and lamellae, and is accompanied by α_2 precipitates. Different morphologies of the $\tau_2 + \alpha_2$ colonies were found to differ in chemical composition, coarse particles being depleted in titanium, and the fine particles enriched in it. The combination of EPMA and EBSD in scanning electron microscopy proved to be very effective in local phase identification of specimens with fine multiphase structure.

1. Introduction

Titanium aluminides are promising materials for aerospace engineering due to their low density and high melting point [1]. Improvement of the properties of γ-base titanium aluminides can be achieved by microstructure optimization through appropriate heat treatment and alloying [2–4]. It is known that the duplex structure can be obtained in binary titanium aluminides after furnace cooling from the α or $\alpha + \gamma$ fields [5]. Such structure provides the optimal combination of mechanical properties [6]. The effect of ternary additions such as Nb, V, Cr, C, Si on microstructure formation is being widely investigated [4]. Iron is also a promising candidate due to the presence of several cubic ternary and quasibinary phases in Al-Ti-Fe system [7], but its effect is less examined. Equilibrium structures of the Al-Ti-Fe system at 800, 900, 1000 °C were studied [7, 8], while the technologically important non-equilibrium structures in the Al-Ti-Fe system (such as, duplex or duplex based) have not been examined at all. Accordingly, the object of the present research is microstructural characterization of the γ-TiAl base alloy with iron addition, after annealing in $\alpha + \gamma$ field and furnace cooling. For this purpose the combination of electron probe x-ray microanalysis (EPMA) and electron backscatter diffraction (EBSD) techniques in scanning electron microscopy (SEM) was employed. This combination is convenient for local chemical and structural characterization for specific morphological features in the specimen. The high lateral resolution of EPMA and EBSD coupled with the large analyzed area available in SEM study, enables comprehensive characterization of specific phases to be made. Bulk structural characterization was performed by x-ray diffraction (XRD). The same specimen is used in all three techniques after a simple preparation procedure.

2. Experimental procedure

2.1. Sample preparation

The investigation was carried out on an Ti-49.6Al-1.9Fe alloy. Specimens were produced by Duriron, Ohio. As-received specimens in the form of 19 mm diameter rods were prepared by induction melting and subsequent hot isostatic pressing (HIP) at 1260 °C, 240 min, 172.4 MPa. The as-received specimens were subjected to metallographical investigation to ensure that no evidence of the as-cast dendritic structure is remained.

The as-received specimens were heat treated above the $\alpha \rightarrow \gamma$ transition temperature: holding at 1400 °C for 40 min followed by furnace cooling (approximately 10 K/min). For the heat treatment a 15–20 mm thick sample was cut from the rod. After the treatment, the sample was halved and its oxide free core was examined.

For characterization, the specimens were ground on SiC grinding paper starting with 120 grit, followed by 240, 320, 400 and 600 grit. Primary polishing was carried out on a wet fabric using alumina slurry with 0.3 μm particle size, and final polishing on a wet fabric. Samples were etched in a solution of 24 ml H_20, 50 ml

Glycerol, 24 ml HNO_3, 2 ml HF, and the etched surface subjected to SEM examination.

2.2. Analytical techniques

2.2.1. Electron backscatter diffraction (EBSD)

Formation of the EBSD pattern is described elsewhere [9–11]. The focused incident electron beam is scattered quasi-elastically within a small interaction volume immediately under the sample surface. The subsequent diffraction of the divergent electrons by the crystal planes forms an array of Kikuchi cones, whenever the Bragg condition is satisfied. Intersection of these cones by the recording screen yields the EBSD pattern. It can be shown that this pattern reflects the symmetry inherent in the crystal, so that analysis of the pattern symmetry yields that of the crystal. The interpretation of the EBSD pattern includes indexing of the crystal planes and directions (observed as bright bands and their intersections respectively).

The EBSD patterns were obtained and analyzed with the aid of a LINK OPAL (Oxford Instruments, UK) device mounted on a high-resolution, field emission gun, digital scanning electron microscope Leo 982 (cooperation Zeiss - Leica). The measurements were carried out under the following conditions: accelerating voltage - 20 kV, beam current - 3 nA, working distance - 17–23 mm, angle between electron probe and sample normal - 70°, probe diameter 40 nm. Initially, the sample surface was examined in the conventional SEM mode and the morphological features of interest were selected. After that the electron probe was localized sequentially on the selected points and the EBSD patterns were captured and solved with the aid of the standard LINK OPAL software package. For calibration of the angular distances between bands, the EBSD pattern from a (001) Si reference single crystal mounted directly on the surface of the sample was used.

2.2.2. Electron probe microanalysis (EPMA)

The electron probe microanalysis was carried out on a JSM 840 (JEOL, Japan) SEM equipped with an energy dispersive LINK ISIS (Oxford Instruments, UK) spectrometer (EDS). The spectrometer allows reliable detection of elements starting with boron.

EDS measurements were carried out at accelerating voltage 10 kV, probe current 1–3 nA, working distance 15 mm, x-ray take-off angle 30°, probe diameter 0.5 μm. Acquisition time was 100 s per point. The standards and analytical lines used for the measurements were as follows: for Al-Al_2O_3, Al K_α, for Ti - bulk Ti, Ti K_α, for Fe - bulk Fe, Fe K_α. Data quantification was based on the conventional correction procedure included in the LINK ISIS software.

Final results for a given phase or morphological feature were normalized to 100% and averaged over a number (usually 5–10) of measurements.

2.2.3. X-ray diffraction (XRD)

XRD analysis was carried out for primary phase identification in the specimen, and its results were correlated with those of the local chemical and structural characterization.

The measurements were carried out on a KW-1810 powder diffractometer (Philips, Holland). Measurement parameters were as follows: Cu K_α radiation, accelerating voltage 40 kV, tube current 40 mA.

Diffraction patterns were obtained from polished specimens in the step mode with step size 0.01° (2θ scale) and 10 s per step exposure.

3. Results and discussion

An optical microphotograph of the alloy structure is presented in Fig. 1. One can see equiaxed grains (marked as '1' in the Fig. 1) and lamellae ('2' in the Fig. 1) similar to that reported for near-equiatomic

Figure 1 Optical microphotograph of the structure formed in Ti-49.6Al-1.9Fe alloy after 1400°C/40 min and furnace cooling: 1- equiaxed grain; 2 - lamellae; 3- black 'grains'.

binary alloys [5]. The microphotograph also reveals an additional morphological feature - black 'grains' (marked '3' in the Fig. 1) in the vicinity of the grain boundaries.

Enlarged SEM images of the black 'grains' are presented in Fig. 2. As can be seen from Fig. 2a (secondary electrons mode), the 'grain' is in fact a colony consisting of particles of different sizes, with the coarse particles forming in the periphery and the fine ones mostly in the central part. In Fig. 2b the colony is imaged in backscattered electrons (compositional contrast mode). White and black particles of different sizes can be distinguished, marked "1" and "2" respectively. EPMA examination (see Table I) revealed that the white particles are enriched in iron relative to its average content in the matrix, and the black particles in titanium. The titanium enrichment is more pronounced in the fine than in the coarse black particles. The titanium content of the fine white particles is also larger than in the coarse ones.

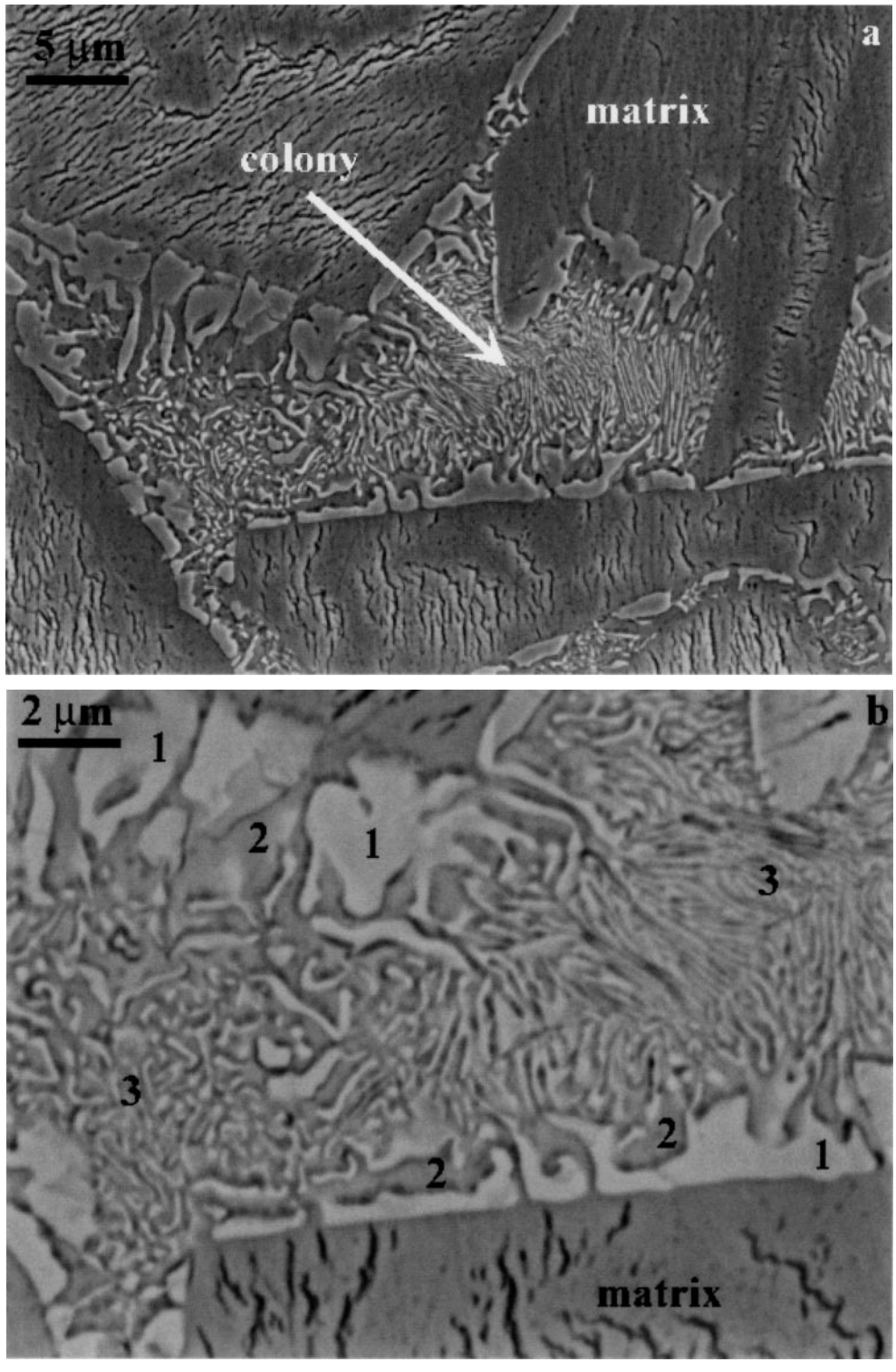

Figure 2 SEM microphotographs of the grain boundary precipitates. (a) - secondary electrons (b) - backscattered electrons (compositional contrast mode). The chemical compositions of the morphological features are presented in the Table I: 1 - coarse white particles; 2 - coarse black particles; 3 - the mixture of the fine black and white particles.

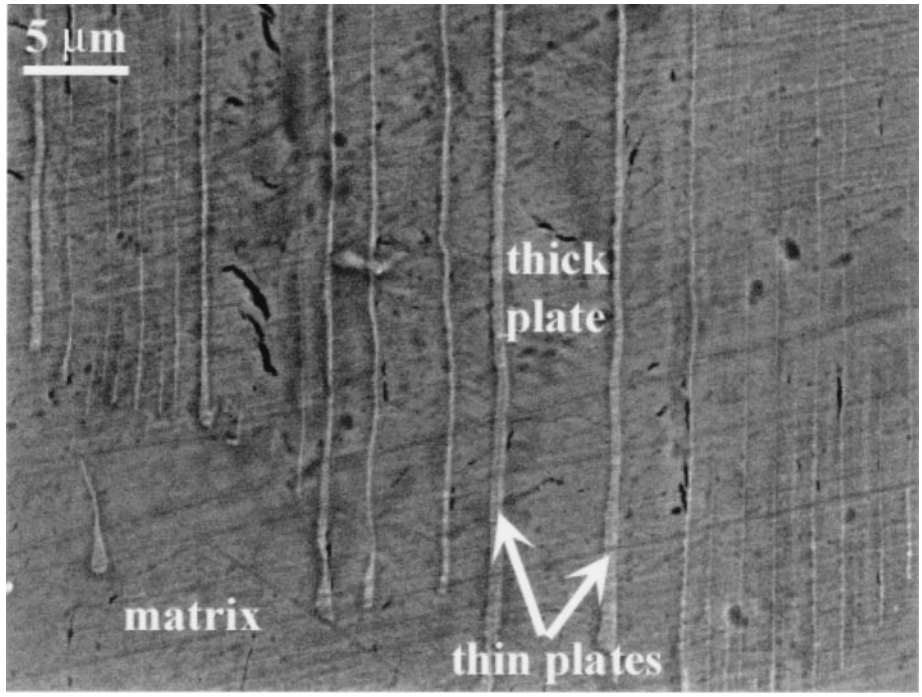

Figure 3 SEM image of lamellae (secondary electrons).

The SEM image of lamellae is presented in Fig. 3. One can distinguish the thin and thick plates. The chemical composition of the thick plates (Table I) is the same as that of the matrix; that of the thin plates could not be measured correctly due to their small width (less than 0.5 μm).

The XRD spectrum of the specimen is presented in Fig. 4. The observed peaks were identified as belonging to either the γ (AuCu type, $a = 0.3998$ nm, $c = 0.4076$ nm [12]), or α_2 (Ni_3Sn type, $a = 0.5793$ nm, $c = 0.4655$ nm [12]) or τ_2 ($Mn_{23}Th_6$ type, $a = 1.2$ nm [7]) phases present in the Al-Ti-Fe system [7].

To identify the morphological features observed, one has to compare their composition measured by EPMA with that of the XRD-detected γ, α_2, τ_2 phases reported in literature (see Table II). Based on data presented in Tables I and II, matrix grains and thick plates were identified as γ, white particles (both coarse and fine) as τ_2 phase. The fine black particles can be recognized as α_2. The observed iron excess (4%) apparently can be explained by influence of the neighboring iron rich τ_2 particles.

TABLE I Chemical composition of observed morphological features measured by EPMA

	Measured Composition, % at.		
Morphological feature	Al	Ti	Fe
matrix grains	53.3 ± 0.5	44.8 ± 0.5	1.8 ± 0.2
thick plates (Fig. 3)	53 ± 0.5	45 ± 0.5	2 ± 0.2
thin plates (Fig. 3)	—	—	—
coarse white particles ("1" in Fig. 2b)	37 ± 0.5	42 ± 0.5	21 ± 0.5
coarse black particles ("2" in Fig. 2b)	39 ± 0.5	59 ± 0.5	2 ± 0.5
fine white particles	32 ± 1	46 ± 1	22 ± 1
fine black particles	29 ± 1	67 ± 1	4 ± 1

TABLE II Chemical composition of γ, α_2 and τ_2 phases reported in literature

	Reported composition, % at.			
Phase	Al	Ti	Fe	Comments
γ	58–42.5	40–55	up to 2.5	composition at 800 °C[7]
α_2	32.5–20.5	66–78	up to 1.5	composition at 800 °C[7]
α_2	39	59	up to 1	maximum Al content reported for 1125 °C[13], iron solubility reported for 1000 °C[7]
τ_2	24.6–47.8	47.8–30.8	21.4–24.5	composition at 800 °C[7]

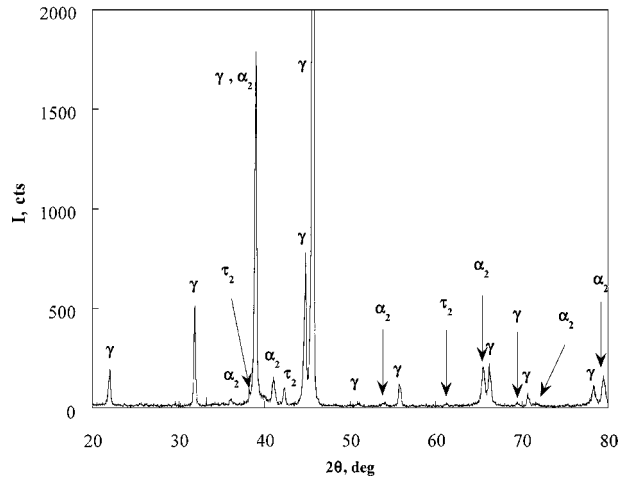

Figure 4 XRD spectrum obtained from Ti-49.6Al-1.9Fe alloy after 1400°C/40 min and furnace cooling.

The coarse black particles exhibit a composition which corresponds to that of α_2 at 1125°C with maximum aluminum content [13], which is beyond the range of existence of α_2 at lower temperatures. Identification of the thin plates was impossible at this stage.

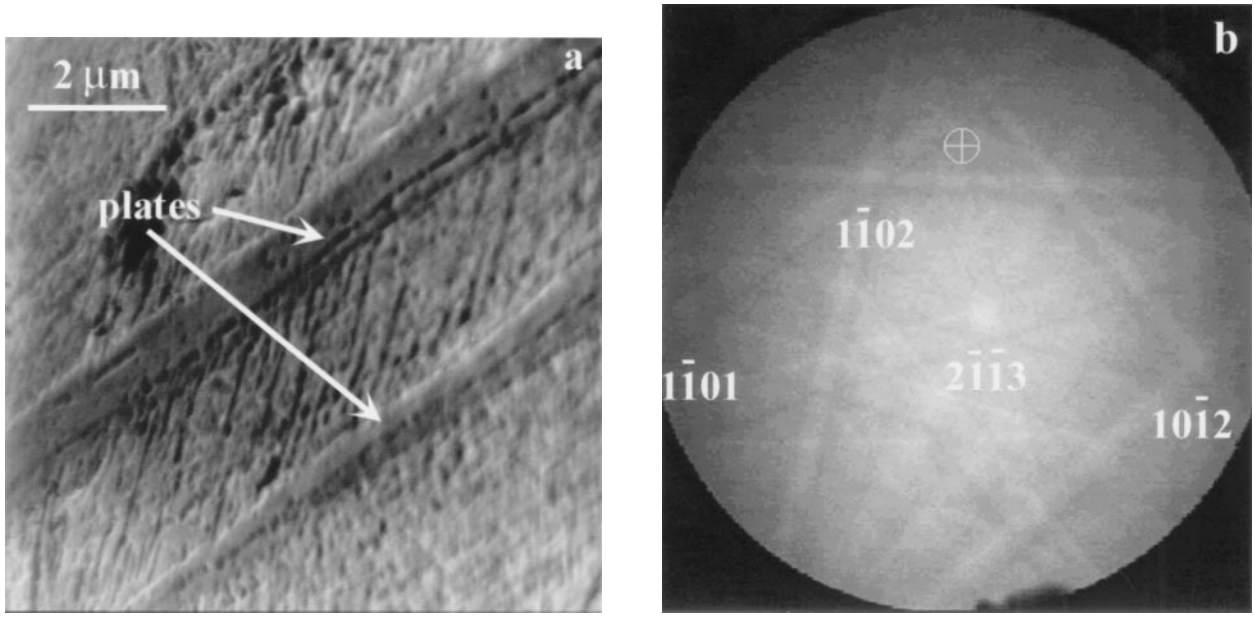

Figure 5 A typical SEM image and the corresponding EBSD pattern from the thin plate.

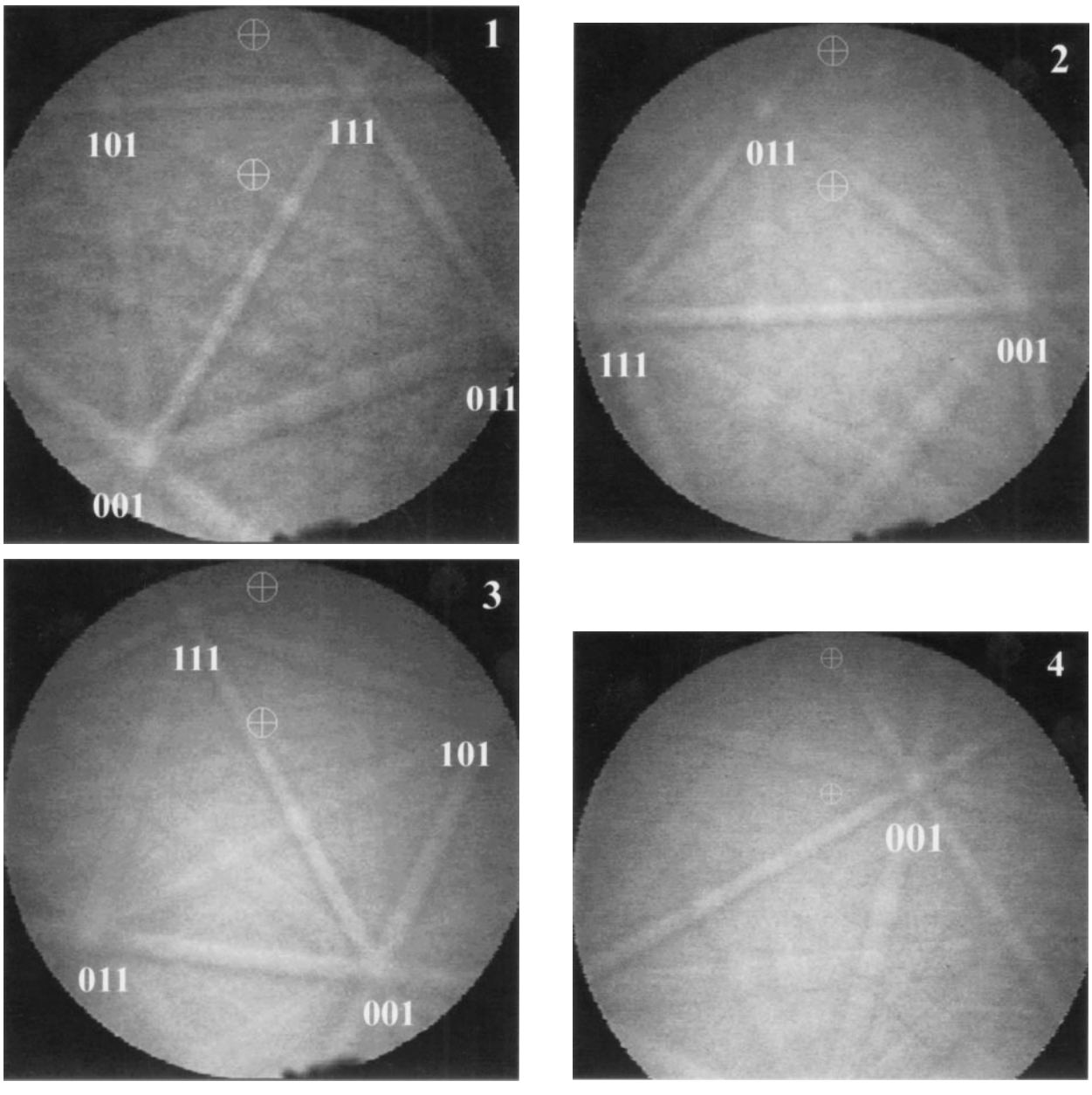

Figure 6 SEM image of colony and corresponding EBSD patterns. (*Continued*)

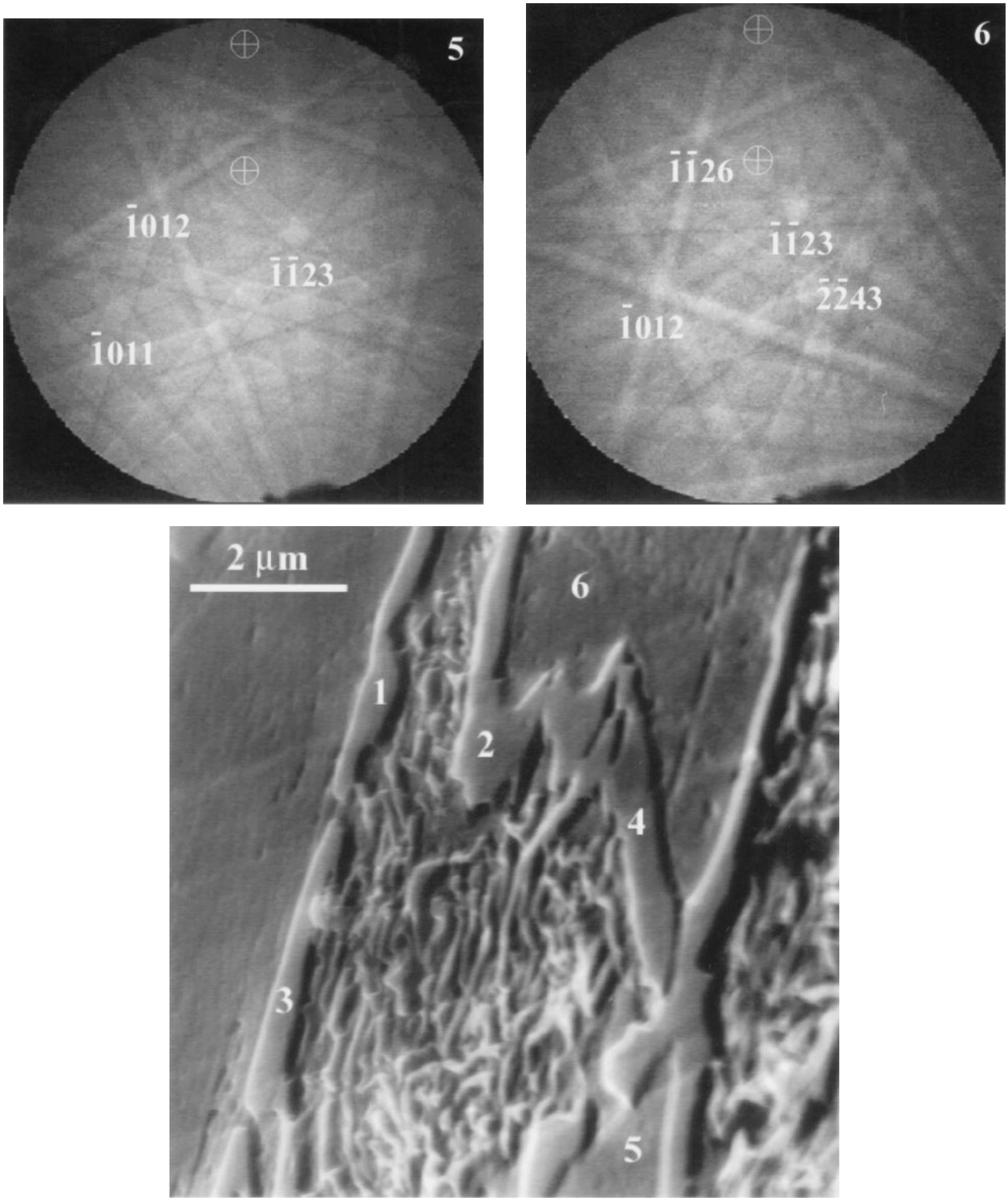

Figure 6 (*Continued*).

It should be noted that the XRD pattern obtained from the specimen contains strong α_2 reflections. Apparently the fine black particles recognized as α_2 cannot be the source of these reflections due to their small amount.

To complete the recognition of the observed morphological features the specimen was examined by EBSD. A typical SEM image of a thin plate and the corresponding EBSD pattern are presented in Fig. 5. Solution of the different patterns captured from the thin plates revealed that the thin plates are α_2-phase. Thus, the observed lamellae consist of alternating γ and α_2 plates. This conclusion is consistent with results reported for the binary Ti-Al alloys after similar heat-treatment [6]. One also concludes that the thin plates are responsible for the strong α_2 peaks observed in the XRD spectrum.

A SEM image of the colony and the corresponding EBSD patterns are presented in Fig. 6. The patterns obtained from points 1–4 were identified as τ_2, and those obtained from points 5 and 6 as α_2. Obviously, points 1–4 correspond to the coarse white particles in Fig. 2b while 5 and 6 correspond to the coarse black ones.

The $\tau + \alpha_2$ colonies are formed during the decomposition of high temperature iron-rich β-Ti [14]. The

coarse particles are formed at higher temperature than fine ones. The composition of coarse α_2 particles implies that the lowest temperature limit of their formation can be estimated as $\sim$1100°C.

4. Conclusions

- The combination of EPMA and EBSD in scanning electron microscopy proved to be very effective in local phase identification of specimens with fine multiphase structure.
- The microstructure of the Ti-49.6Al-1.9Fe alloy after annealing at 1400°C for 40 min and furnace cooling consists of γ, $(\gamma + \alpha_2)$ lamellae and colonies of the $\alpha_2 + \tau_2$ precipitates on the grain boundaries.
- The ternary τ_2 phase found in the specimen contains 21–22 at. % of iron.
- The fine particles (both α_2 and τ_2) in the colonies are enriched in titanium relative to the coarse ones.
- The coarse α_2 particles in colonies are enriched in aluminum in comparison to the equilibrium Al solubility at room temperature.

References

1. F. H. FROES, C. SURYNARAYNA and D. ELIEZER, *Journal of Materials Science* **27** (1992) 5113.
2. Y-W. KIM and F. H. FROES in "High Temperature Aluminides and Intermetallics" edited by S. H. Whang, C. T. Liu, D. P. Pope and O. J. Stiegler (TMS Warrendale, Pennsylvania, 1990) p. 465.
3. J. BEDDOES *et al*., *International Materials Reviews* **40** (1995) 197.
4. SH.-CH. HUANG, in "Structural Intermetallics," edited by R. Darolia, *et al*., (The Minerals, Metals & Materials Society, 1993) p. 167.
5. S. A. JONES and M. J. KAUFMAN, *Acta Metall. Mater*. **41** (1993) 387.
6. SH.-CH. HUANG, *Metallurgical Transactions A* **23A** (1992) 375.
7. M. PALM, G. INDEN and N. THOMAS, *Journal of Phase Equilibria* **16** (1995) 209.
8. M. PALM, A. GORZEL, D. LETZIG and G. SAUTHOFF, in "Structural Intermetallic," edited by M.V. Nathal *et al*., (The Minerals, Metals & Materials Society, 1997) 885.
9. D. J. DINGLEY and V. RANDLE, *Journal of Materials Science* **27** (1992) 4545.
10. Link Opal Operator's Guide. Oxford Instruments, Microanalysis Group, Issue 1 (1995).
11. D. J. DINGLEY, K. Z. BABA-KISHI and V. RANDLE, "Atlas of Backscattering Kikuchi Diffraction Patterns, Microscopy in Materials Science Series" (Institute of Physics Publishing, Bristol and Philadelphia, 1995).
12. P. VILLARS and L. D. CALVERT, "Pearson's Hamdbook of Crystallographic Data for Intermetallic Phases," Vol. 2 (American Society of Metals, Metals Park Ohio, 1985) p. 1075.
13. "Phase Diagrams of Binary Titanium Alloys," edited by J. L. Murray (Metals Park, Ohio 44073, 1987) p. 12.
14. L. LEVIN, A. TOKAR, M. TALIANKER and E. EVANGELISTA, *Intermetallics* **7** (1999) 1317.

Received 12 March 1999
and accepted 8 February 2000